Electronic Supplementary Material (ESI) for Chemical Communications

Discrimination of nerve gases mimics and other organophosphorous derivatives in gas phase using a colorimetric probe array.

Katherine Chulvi,[a,b] Pablo Gaviña,[a,b] Ana M. Costero,[a,b] Salvador Gil,[a,b] Margarita Parra,[a,b] Raúl Gotor,[a,b] Santiago Royo,[a,c,d] Ramón Martínez-Máñez,[a,c,d] Felix Sancenón[a,c,d] and José-L. Vivancos[a,d,e]

[a] Centro de Reconocimiento Molecular y Desarrollo Tecnológico (IDM),Unidad Mixta Universidad Politécnica de Valencia-Universitat de Valencia
[b] Departamento de Química Orgánica, Universitat de Valencia, Dr.Moliner, 50, 46100 Burjassot (Valencia). Teléfono: 963543151. E-mail: ana.costero@uv.es.
[c] Departamento de Química, Universidad Politécnica de Valencia Camino de Vera s/n, 46022, Valencia, Spain.
[d] CIBER de Bioingeniería, Biomateriales y Nanomedicina (CIBER-BBN)
[e]Departamento de Proyectos de Ingeniería, UniversitatPolitècnica de Valencia, Camino de Vera s/n, 46021, Valencia, Spain.

Supporting Information

Materials and General Procedures

All reagents and dyes **2-4**, **7**, **8**, **12**, **15** and **16** were commercially available and were used without further purification. Dyes **6**,[S1] **10**,[S2] **11**[S3] and **14**[S4] were synthesized according to previously published procedures.

^{1}H and ^{13}C NMR spectra were recorded on a Bruker DPX300 (300 MHz) or a Bruker AV400 (400 MHz) NMR spectrometer. All measurements were carried out using the residual solvent peak as the internal reference. High-resolution mass spectra were recorded in the positive ion mode on a VG-AutoSpec.

TLC plates used as solid supports for the colorimetric arrays were commercially available silica gel on TLC Al foils (5 cm x 5 cm) without fluorescence indicator (Sigma-Aldrich). A HP Laser Jet M1005 MFP scanner was used to obtain pictures of the arrays.

Syntheses:

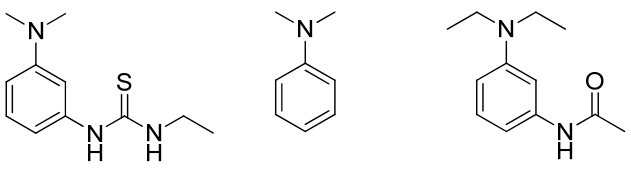

Figure S1. Dialkylanilines used in the diazonium coupling reactions.

N-[3-(dimethylamino)phenyl]-N'-ethyl thiourea, **17**. A mixture of N,N-dimethyl-*m*-phenylenediamine (1.33 g, 9.8 mmol), ethyl isothiocyanate (0.86 mL, 9.8 mmol) and Et_3N (1.36 mL, 9.8 mmol) in THF (10 mL) was refluxed for 13 h. Evaporation of the solvent and Et_3N under reduced pressure led to a slightly yellow crystalline solid (1.91 g, 91%) which was used without further purification. ^{1}H-NMR (300 MHz, $CDCl_3$): δ 7.95 (s, 1H, NH), 7.28 – 7.21 (m, 1H), 6.62 (dd, *J* = 8.4 and 2.5 Hz, 1H), 6.54 – 6.49 (m, 1H), 6.47 (t, *J* = 2.2 Hz, 1H), 6.20 (br.s, 1H, NH), 3.66 (m, 2H), 2.95 (s, 6H), 1.18 (t, J = 7.2 Hz, 3H). ^{13}C-NMR (75 MHz, $CDCl_3$): δ 180.49, 152.17, 137.37, 130.92, 112.68, 111.34, 108.90, 40.69, 30.07, 14.75.

Azo dyes. Azo dyes **1**, **5**, **9** and **13** were synthesized by a coupling reaction between the diazonium ion obtained from 4-aminopyridine (or its 3-bromo- or 2,6-dichloro derivatives) and the corresponding dialkylaniline (Figure S1). A typical procedure is described for the synthesis of compound **5**.

Compound 5. 4-amino-2,6-dichloropyridine (166 mg, 1.0 mmol) was dissolved in a mixture of 85% phosphoric acid (1 mL) and 68% nitric acid (0.5 mL). The solution was cooled to 0 ºC with an ice-bath and sodium nitrite (76 mg, 1.1 mmol) was added slowly. Then 4 g of crushed ice were added and the mixture was stirred for 1 h. The resulting yellow solution containing the diazonium salt was added dropwise over a mixture of N,N-dimethylaniline (**18**) (127 µL, 1.0 mmol), potassium acetate (2.1 g), sodium carbonate (1.8 g) and acetic acid (1.3 g) in water (30 mL) at 0 ºC and the solution was stirred at this temperature for 12 h. The red-purple precipitate was collected by filtration, washed thoroughly with water and dried at 70 ºC in an oven to yield **5** as a deep-red crystalline solid (235 mg, 79 %). ^{1}H NMR (300 MHz, $CDCl_3$): δ 7.83 (d, *J* = 9.3 Hz, 1H), 7.54 (s, 1H), 6.68 (d, *J* = 9.4 Hz, 1H), 3.09 (s, 3H). ^{13}C NMR (75 MHz, $CDCl_3$): δ 162.12, 154.57, 151.49, 143.64, 127.45, 115.95, 112.05, 40.79. HRMS (EI): *m/z* calcd. for $C_{13}H_{12}N_4Cl_2$ ($[M+H]^+$), 295.0517; found, 295.0518.

Compound 1. Deep purple solid (99 mg, 34 %). ^{1}H NMR (300 MHz, $CDCl_3$): δ 8.55 (dd, *J* = 4.8, 1.4 Hz, 2H), 7.72 (d, *J* = 9.3 Hz, 1H), 7.47 (d, *J* = 6.2 Hz, 2H), 7.20 (s, *J* = 1.2 Hz, 1H), 6.45 (dd, *J* = 9.3, 2.8 Hz, 1H), 3.67 – 3.54 (m, 2H), 3.10 (s, 6H), 1.25 (t, *J* = 7.2 Hz, 3H). ^{13}C NMR (75 MHz, $CDCl^3$): δ 180.26, 158.52, 154.77, 150.62, 138.91, 132.93, 116.57, 116.09, 108.49, 102.36, 45.44, 41.30, 14.49. HRMS (EI): *m/z* calcd. for $C_{16}H_{21}N_6S$ ($[M+H]^+$), 329.1470; found, 329.1475.

Compound 9. Dark purple solid (1.4 g, 41 %). ^{1}H NMR (300 MHz, DMSO-d_6): δ 10.61 (br. s, 1H, NH), 8.78 (d, *J* = 6.8 Hz, 2H), 8.13 (d, *J* = 7.0 Hz, 2H), 7.94 (d, *J* = 2.7 Hz, 1H), 7.84 (d, *J* = 9.7 Hz, 1H), 6.79 (dd, *J* = 9.7 and 2.8 Hz, 1H), 3.57 (q, *J* = 6.9 Hz, 4H), 2.26 (s, 3H), 1.22 (t, *J* = 7.0 Hz, 6H). ^{13}C NMR (75 MHz, DMSO-d_6): δ 169.77, 162.03, 155.12, 143.40, 142.84, 133.27, 124.43, 117.29, 110.02, 100.73, 45.37, 25.05, 12.72. HRMS (EI): *m/z* calcd. for $C_{17}H_{21}N_5O$ ($[M+H]^+$), 312.1824; found, 312.1826.

Compound 13. Dark purple solid (465 mg, 66%). ^{1}H NMR (300 MHz, DMSO-d_6): δ 11.26 (br. s, 1H, NH), 8.99 (s, 1H), 8.59 (d, *J* = 6.1 Hz, 1H), 8.05 (d, *J* = 2.6 Hz, 1H),

7.94 (d, *J* = 6.0 Hz, 1H), 7.78 (d, *J* = 9.6 Hz, 1H), 6.83 (dd, *J* = 9.6 and 2.7 Hz, 1H), 3.58 (q, *J* = 7.0 Hz, 4H), 2.27 (s, 3H), 1.22 (t, *J* = 7.0 Hz, 6H). ^{13}C NMR (75 MHz, DMSO-d_6): δ 170.17, 157.55, 154.89, 148.14, 144.45, 140.65, 133.25, 129.84, 118.07, 112.09, 110.07, 100.46, 45.46, 25.58, 12.71. HRMS (EI): *m/z* calcd. for $C_{17}H_{20}N_5OBr$ ([M]+), 390.0924; found, 390.0918.

Selection of the dyes and detection experiments

A large number of commercially available dyes and some dyes reported by us were selected and tested in the presence of organophosphorous compounds shown in Scheme 2. In many cases no response was observed, the response was poor or not reproducible. From these studies finally the set of 16 dyes included in the manuscript was selected. A closer look to the dyes show that some of them are push-pull chromophores containing active reactive sites such as alcohol, amine, pyridine groups which are known to react with organophosphorous derivatives via nucleophilic attack to the phosphorous atom (see dyes 1, 2, 3, 5, 6, 7, 9, 10, 11, 13, and 14). Moreover other dyes used (i.e dyes 1, 4, 8, 9, 12, 13, 15 and 16) were also included in the array and displayed colour modulation most likely due to coordination or reaction with hydrolysis products of organophosphorous derivatives such as fluoride, cyanide, phosphate and protons.

In a typical sensing experiment, a 50 μL drop of the corresponding organophosphorous derivative (or conc HCl) was deposited in the bottom of a 9 cm diameter Petri dish (110 mL volume). The colorimetric probe array was fixed in the top of the dish which was then closed. The temperature of the environment was kept at 25 ºC. After 30 minutes the array was taken out of the Petri dish, scanned and compared with a control array not exposed to the tested vapour and kept at the same temperature.

Vapour pressures and saturated vapour concentration of the studied analytes

	Vapor pressure (mm Hg)	*Saturated vapour concentration* (ppm v/v)
DCNP	0.158[(a)] (25ºC)	208
DFP	0.579[(a)] (20ºC)	762
DCP	0.1[(a)] (25ºC)	132
EDCP	0.886[(b)] (25ºC) 1.38[(c)] (25ºC)	1166 1816
DPEP	0.000359[(d)] (25ºC)	0.47
DMTMP	0.029[(b)] (25ºC) 0.012[(c)] (25ºC)	38.2 15.8
DCTP	0.5[(a)] (25ºC)	658
DOPP	0.010[(b)] (25ºC) 0.0096[(d)] (25ºC)	13.2 12.6

[(a)] Experimental value
[(b)] Predicted value (ACD/Labs)
[(c)] Predicted value (EPI Suite mean value from Antoine and Grain methods)
[(d)] Predicted value (EPI Suite modified Grain method)

Interference studies with NO_x and CO_2.

Experiments with these two interferents were carried out following the procedure describes above. CO_2 was generated from 2 mg dry ice and NO_x was obtained from the reaction between nitric and sulphuric acid in atmospheric air. Then a known volume of the gas at atmospheric pressure and 25ºC was injected in the Petri dish containing the array.

Studies at different concentrations of DFP

The experiments were carried out by flash evaporation of 1 μL of DFP in a round bottom flask of known volume (1.3, 2.5, 3.2, 3.6 and 5.7L) where the array had been previously placed. Normal air was let enter inside until atmospheric pressure. The closed system was then left at 25ºC for 30 minutes. Concentrations of DFP of 108, 54, 44, 39, 24 ppm (v/v) were tested and colour changed in the array were analysed as explained above. A PLS prediction model for prediction of the DFP concentration was created with the RGB colour coordinates obtained from the chromogenic array (*vide infra*).

Statistical Multivariate Analysis

All multivariate analyses were carried out with Matlab (Version 7.8.0.R2009a, MathWorks). We have included a third method of KNN classification where the "k" closest samples in a reference set vote on the class of an unknown sample based on distance to the reference samples. If no majority is found, the unknown is assigned the class of the closest sample. K-nearest neighbour classifier (KNN) models include the probabilities of each sample belonging to each possible class in the model classification probability field. The probability that a sample belongs to class ‘A’ is calculated as the fraction of nearest-neighbours which have that particular class. The number of components was used as default (i.e. the rank of analytes). Principal components analysis (PCA) was carried out with the Solo 6.2 software (eigenvector Research Incorporated, WA, USA). Autoscale preprocessing and singular value decomposition (SVD), i.e., an algorithm, were used to obtain a general solution to the problem of finding pseudoinverses. PLS is a multivariate projection method that models the relation between and array of dependent variables (Y) and another array of independent variables (X). The principle of the technique PLS is to find the components of the matrix of input (X) that describe, as much as possible, relevant variations in the input variables, and at the same time get the highest correlation with the objectives (Y), giving the minor weight to the variations that are irrelevant or relate to noise. PLS attempts to find factors (called Latent Variables) that maximize the amount of variation explained in X that is relevant for predicting Y. Preprocessing used is the Autoscale and the Cross validation: contiguous block is used to obtain Latent Variables. PLS prediction model of DFP was created with the colour coordinates obtained from the chromogenic arrays.

Principal Component Analysis (PCA):

Tables below correspond to PCA analysis for organophosphorous derivatives DFP, DCP, DCNP, EDCP, DPEP, DMTMP, DCTP, DOPP and HCl (see Figure 2 in the manuscript for a representation of the PCA graphic).

Eigenanalysis of the Correlation Matrix

	Eigenvalues	Variance Captured (%)	Cumulative Variance Captured (%)
1	2.48E+01	5.16E+01	51.64
2	5.59E+00	1.17E+01	63.29
3	4.42E+00	9.21E+00	72.50
4	3.50E+00	7.29E+00	79.79
5	2.54E+00	5.29E+00	85.08
6	1.46E+00	3.05E+00	88.13
7	1.21E+00	2.52E+00	90.65
8	8.88E-01	1.85E+00	92.50
9	7.27E-01	1.51E+00	94.02
10	7.08E-01	1.48E+00	95.49
11	4.70E-01	9.79E-01	96.47
12	3.89E-01	8.11E-01	97.28
13	3.34E-01	6.95E-01	97.98
14	2.28E-01	4.76E-01	98.45
15	1.66E-01	3.47E-01	98.80
16	1.35E-01	2.82E-01	99.08
17	1.11E-01	2.30E-01	99.31
18	8.48E-02	1.77E-01	99.49
19	6.41E-02	1.34E-01	99.62
20	4.53E-02	9.44E-02	99.72

Sensor	Variable	PC 1 (51.64%)	PC 2 (11.65%)	PC 3 (9.21%)	PC 4 (7.29%)	Q Residuals (20.21%)	Hotelling T^2 (79.79%)
	R	-7.19E-02	3.77E-02	-1.29E-01	4.34E-02	20.3764552	1.17974242
1	G	7.20E-03	3.12E-01	-5.80E-02	-1.51E-01	9.35004246	5.80744056
	B	-5.25E-02	3.12E-01	-1.02E-01	2.07E-01	4.95047543	7.21446676
	R	7.58E-02	1.56E-01	2.13E-01	-2.95E-02	13.4706056	3.58495926
2	G	1.85E-01	6.40E-02	-2.66E-02	-4.15E-02	3.15994683	1.91167583
	B	1.93E-01	7.05E-02	-6.67E-02	4.51E-03	0.64254918	2.20250784
	R	1.79E-01	1.45E-01	9.94E-02	2.67E-02	1.12544878	2.98684358
3	G	4.98E-02	3.64E-01	1.38E-02	6.79E-02	4.65930074	6.58095835
	B	-1.83E-01	4.60E-03	-1.52E-01	1.16E-01	0.63056944	3.29013168
	R	-1.97E-01	3.51E-02	3.55E-03	-8.64E-02	0.20993836	2.22777206
4	G	1.69E-01	-1.81E-01	-2.59E-02	-6.31E-02	2.4689863	3.09454651
	B	-1.73E-01	-1.26E-01	5.05E-02	-1.61E-01	1.6569702	3.49584844
5	R	6.15E-02	-7.53E-02	-8.10E-02	-2.63E-01	15.6719409	4.01203021

Sensor	Variable	PC 1 (51.64%)	PC 2 (11.65%)	PC 3 (9.21%)	PC 4 (7.29%)	Q Residuals (20.21%)	Hotelling T^2 (79.79%)
	G	1.87E-01	1.02E-01	-8.50E-02	3.67E-03	1.03491916	2.4806733
	B	-1.83E-01	1.49E-01	-8.59E-03	-4.68E-03	1.06821558	2.63272004
	R	1.86E-01	4.81E-02	2.45E-03	1.69E-01	0.79482527	3.07120595
6	G	8.12E-02	1.50E-01	2.27E-01	2.10E-01	8.5149751	5.874542
	B	1.81E-01	5.73E-02	-3.85E-03	1.22E-01	2.95226567	2.40431628
	R	-6.62E-02	2.50E-01	2.62E-01	-2.12E-01	2.15983742	8.46177804
7	G	1.84E-01	1.37E-01	4.99E-03	1.31E-02	1.35385052	2.48726626
	B	-7.12E-02	4.99E-02	-2.37E-01	2.23E-01	11.3685472	5.34109936
	R	1.39E-01	9.74E-02	-1.95E-01	1.75E-02	7.73679965	3.1627263
8	G	-9.72E-02	-4.30E-02	2.19E-01	-2.00E-01	10.4978488	4.6572014
	B	1.81E-01	3.10E-02	-1.17E-01	-1.47E-01	1.29561833	3.24368291
	R	7.27E-02	-3.45E-02	1.58E-01	3.27E-01	9.81176708	6.5068654
9	G	1.88E-01	6.23E-02	-2.87E-02	1.52E-01	0.49741727	2.969952
	B	-1.85E-01	5.74E-02	-5.90E-02	-9.73E-02	2.23599397	2.37000112
	R	1.81E-01	-3.88E-02	1.72E-01	3.76E-02	1.22293004	3.06475718
10	G	-1.01E-01	1.03E-01	-3.18E-01	-5.35E-02	6.04316039	5.84997072
	B	1.28E-01	2.02E-01	8.37E-03	5.54E-02	9.26321976	2.83876793
	R	1.19E-01	-5.54E-02	-1.12E-01	-4.36E-02	14.7954633	1.49023619
11	G	1.79E-01	1.48E-02	4.67E-02	1.96E-01	1.50155857	3.42998152
	B	-1.67E-01	1.97E-01	-5.66E-02	-2.47E-02	1.98539421	3.30633188
	R	1.75E-01	9.86E-02	2.98E-02	-9.56E-02	4.00615342	2.36102541
12	G	1.83E-01	1.01E-01	-9.47E-02	-5.11E-02	1.71821616	2.59113456
	B	1.63E-01	-8.56E-03	-1.28E-01	-1.84E-01	3.93855248	3.60227967
	R	-4.22E-02	9.62E-02	-3.45E-02	-1.27E-01	21.898378	1.33516181
13	G	1.88E-01	1.10E-01	1.27E-02	-3.49E-02	1.2381234	2.30542785
	B	-1.34E-01	1.08E-01	-2.03E-01	1.39E-01	6.27160748	4.23832101
	R	-1.78E-01	1.44E-01	5.36E-02	1.01E-01	1.23858746	3.08772863
14	G	-1.40E-01	6.84E-02	2.03E-01	2.00E-01	4.28071332	4.9522232
	B	-1.34E-01	1.15E-01	2.09E-01	2.48E-01	1.94395194	6.39176914
	R	-5.32E-02	2.35E-01	-2.77E-01	-2.54E-02	7.27162994	6.36335346
15	G	-4.50E-02	2.26E-01	2.54E-01	-2.83E-01	2.52001489	9.30968541
	B	-3.88E-02	2.89E-01	1.34E-01	-2.55E-01	4.86505742	7.90799827
	R	1.37E-01	-7.12E-02	-8.90E-03	-1.03E-01	12.2481147	1.62243957
16	G	1.40E-01	-1.10E-01	2.71E-01	-1.10E-02	3.08460021	4.96067574
	B	1.75E-01	4.44E-02	-1.58E-01	-1.48E-01	1.15208282	3.73777701

Tables below correspond to PCA analysis for organophosphorous derivatives DFP, DCP, DCNP, EDCP, DPEP, DMTMP, DCTP, DOPP, HCl and interferents (CO_2 and NO_x). Blank samples (without the presence of organophosphorous derivatives or interferents) (three replicates at 25 ^oC), blank samples at different temperatures (0ºand 55ºC) and a blank sample in saturated H_2O (25^oC) have also been included (see Figure S2 below for a representation of the PCA graphic).

Eigenanalysis of the Correlation Matrix

	Eigenvalues	Variance Captured (%)	Cumulative Variance Captured (%)
1	2.17E+01	45.26	45.26
2	5.71E+00	11.90	57.16
3	4.01E+00	8.36	65.52
4	3.26E+00	6.80	72.32
5	2.34E+00	4.87	77.19
6	1.91E+00	3.99	81.18
7	1.43E+00	2.99	84.17
8	1.21E+00	2.53	86.70
9	1.01E+00	2.10	88.80
10	8.79E-01	1.83	90.64
11	7.09E-01	1.48	92.11
12	6.59E-01	1.37	93.49
13	6.22E-01	1.30	94.78
14	4.59E-01	0.96	95.74
15	3.60E-01	0.75	96.49
16	2.66E-01	0.55	97.05
17	2.27E-01	0.47	97.52
18	2.02E-01	0.42	97.94
19	1.85E-01	0.38	98.32
20	1.39E-01	0.29	98.61

Sensor	Variable	PC 1 (45.26%)	PC 2 (11.90%)	PC 3 (8.36%)	PC 4 (6.80%)	Q Residuals (27.68%)	Hotelling T^2 (72.32%)
	R	-7.60E-02	-4.01E-02	2.29E-02	-1.25E-01	32.4857	1.1089
1	G	1.58E-02	-6.68E-02	3.31E-01	4.71E-02	20.9237	5.4644
	B	-6.63E-02	5.30E-02	3.09E-01	-1.60E-01	16.9035	6.0191
	R	1.28E-01	-1.73E-01	1.03E-01	1.66E-01	13.6772	3.9712
2	G	1.84E-01	-1.74E-01	5.37E-02	5.31E-02	2.7996	3.2815
	B	1.97E-01	-1.31E-01	5.83E-02	8.83E-03	1.6755	2.7996
	R	1.73E-01	1.64E-01	1.79E-01	3.99E-03	2.7787	4.1777
3	G	1.97E-02	1.37E-01	4.06E-01	-2.70E-02	8.8175	8.6835
	B	-1.92E-01	-5.04E-02	-6.19E-03	-1.82E-01	2.9899	3.4182
	R	-2.09E-01	-5.11E-02	4.51E-02	2.30E-02	1.0044	2.2984
4	G	1.72E-01	6.83E-02	-2.03E-01	9.93E-03	6.5071	3.5599
	B	-1.94E-01	1.39E-02	-9.66E-02	2.87E-02	5.6144	2.2566
	R	9.51E-02	-1.58E-01	-5.17E-02	5.00E-02	25.6544	1.8479
5	G	1.97E-01	4.65E-03	9.99E-02	-6.70E-02	4.1322	2.5022
	B	-1.83E-01	-9.07E-02	1.78E-01	-2.53E-02	3.9095	3.4768
	R	8.95E-02	3.28E-01	3.04E-02	-1.73E-01	4.3756	6.8866
6	G	-1.66E-02	3.38E-01	1.63E-01	-1.17E-01	7.6371	7.2685
	B	9.85E-02	3.15E-01	4.66E-02	-1.64E-01	5.0032	6.4970
7	R	-1.03E-01	9.27E-02	2.95E-01	2.28E-01	8.1824	7.4162

Sensor	Variable	PC 1 (45.26%)	PC 2 (11.90%)	PC 3 (8.36%)	PC 4 (6.80%)	Q Residuals (27.68%)	Hotelling T^2 (72.32%)
	G	1.95E-01	4.10E-02	1.11E-01	6.30E-02	4.1136	2.6327
	B	-6.77E-02	-5.95E-02	1.93E-03	-8.44E-02	34.2716	0.7175
	R	1.48E-01	-2.65E-02	4.38E-02	-5.72E-02	20.0295	1.3085
8	G	-1.01E-01	3.84E-02	-4.79E-02	3.13E-01	17.6728	5.2644
	B	1.89E-01	-5.78E-02	3.13E-02	-2.78E-02	7.8662	1.9221
	R	4.02E-02	2.54E-01	-8.71E-02	-1.71E-02	22.6201	3.4755
9	G	1.98E-01	9.75E-02	3.01E-02	-3.15E-02	3.4625	2.3794
	B	-1.93E-01	-1.12E-01	8.83E-02	-5.91E-02	3.1516	2.8687
	R	1.53E-01	2.22E-01	-6.73E-03	-2.05E-02	8.4809	3.4252
10	G	-8.18E-02	-1.52E-01	1.38E-01	-3.34E-01	11.2861	7.5431
	B	1.31E-01	6.52E-02	2.24E-01	-6.80E-02	15.3993	3.5888
	R	1.11E-01	-7.10E-03	-7.22E-02	3.60E-03	28.4825	0.8248
11	G	1.76E-01	1.73E-01	-3.55E-02	1.61E-02	5.8599	2.9468
	B	-1.86E-01	2.78E-02	1.91E-01	-1.29E-01	1.8353	4.1597
	R	1.78E-01	-5.67E-02	6.26E-02	1.56E-01	7.8579	2.9736
12	G	1.92E-01	-1.29E-01	6.31E-02	5.02E-02	3.1560	2.8181
	B	1.80E-01	-1.20E-01	2.91E-02	-2.55E-02	8.2865	2.2728
	R	-2.82E-02	-6.35E-02	2.20E-02	1.91E-01	33.5373	1.9683
13	G	1.92E-01	2.00E-02	1.18E-01	6.27E-02	5.0233	2.5926
	B	-7.53E-02	-2.02E-01	1.38E-01	-2.66E-01	13.4367	6.4139
	R	-1.75E-01	8.71E-02	7.76E-02	1.37E-01	8.3420	2.9523
14	G	-1.42E-01	1.97E-01	-1.58E-02	1.89E-01	9.0247	4.4563
	B	-1.54E-01	2.12E-01	3.45E-02	1.40E-01	6.2576	4.2148
	R	8.76E-02	-3.16E-01	1.09E-01	-1.46E-03	8.5636	5.6227
15	G	-6.35E-02	5.06E-02	2.54E-01	3.43E-01	10.2450	8.8537
	B	-2.82E-04	-1.01E-01	2.77E-01	2.39E-01	17.8934	6.7702
	R	1.41E-01	3.30E-02	-7.24E-04	-1.42E-01	19.7223	1.9447
16	G	1.11E-01	1.05E-02	-1.10E-01	2.97E-01	15.7105	5.3111
	B	1.90E-01	-7.41E-02	8.07E-02	-1.12E-01	4.7648	2.8437

Figure S2 shows the resulting PCA for the 9 sampling organo- phosphate and phosphonate derivatives (three replicates), interferents (CO_2 and NO_x, three replicates) and blank samples (three blank samples at 25 ^oC, two blank samples at different temperatures (0º and 55ºC) and one blank sample in saturated H_2O at 25^oC) using all dyes (16 x 3 coordinates/dye). Here the PCs score plot uses two PCs (PC1 and PC2) representing the 57.16% of variance. A clustering of the data was found. A clear discrimination of the nerve agent simulants DCNP, DFP and DCP was observed and this was not confused with the presence of acidic vapours (HCl). Moreover other tested products were gathered in larger clusters which allowed to classify the samples in organo-phosphates (EDCP and DCTP) and phosphonates (DOPP, DMTMP and DPEP). The different blank samples and CO_2 and NO_x also clustered in the same space. This last result indicated that no interference from CO_2 and NO_x or the use of different temperatures or saturated H_2O was observed.

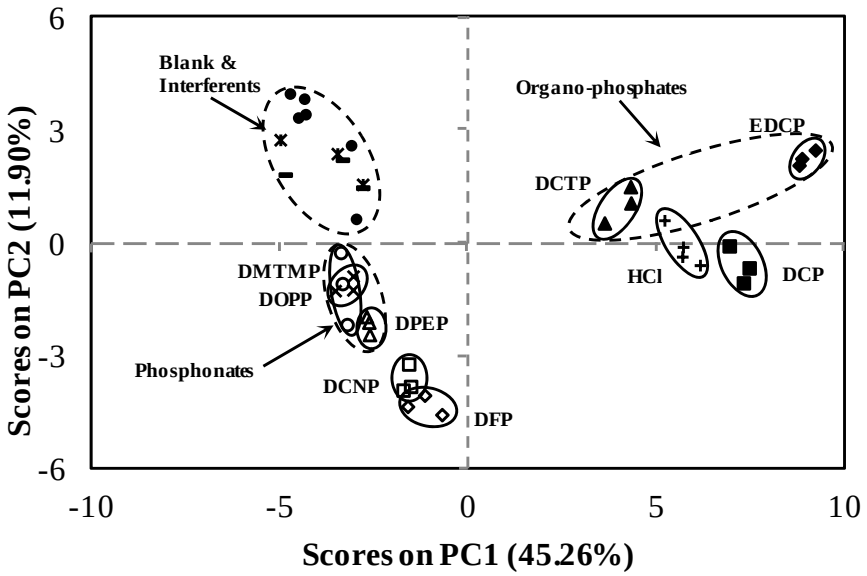

Figure S2. PCA score plot of PC1 and PC2 for some products in Scheme 2 and HCl (3 each) and the trial clustering, blank samples (three blank samples at 25 ^{o}C, two blank samples at 0^{o} and 55^{o}C and one blank sample in saturated H_2O at 25^{o}C) and interferents as CO_2 and NOx have also been included.

Hierarchical Clustering Analysis (HCA):

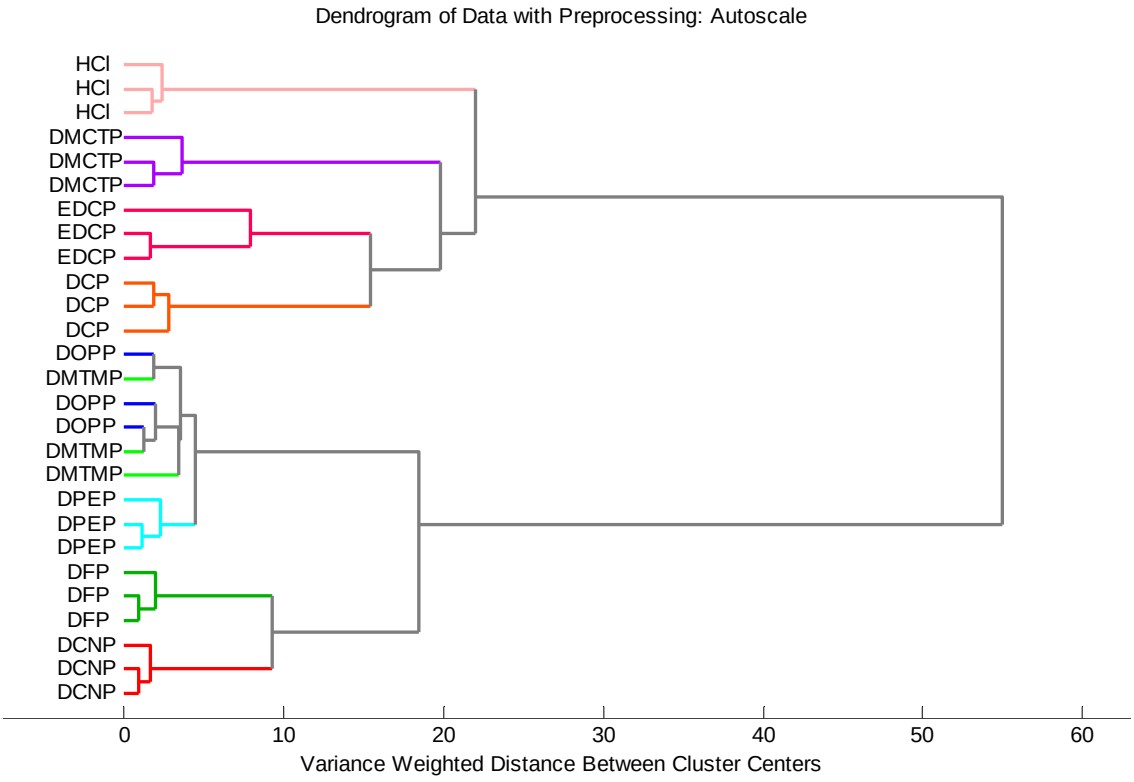

Figure S3. Dendrogram for 9 sampling organo- phosphate and phosphonate derivatives showing Euclidean Distance with Ward Linkage, in this case clustering is done on the seven PCA scores instead of the original X-variables.

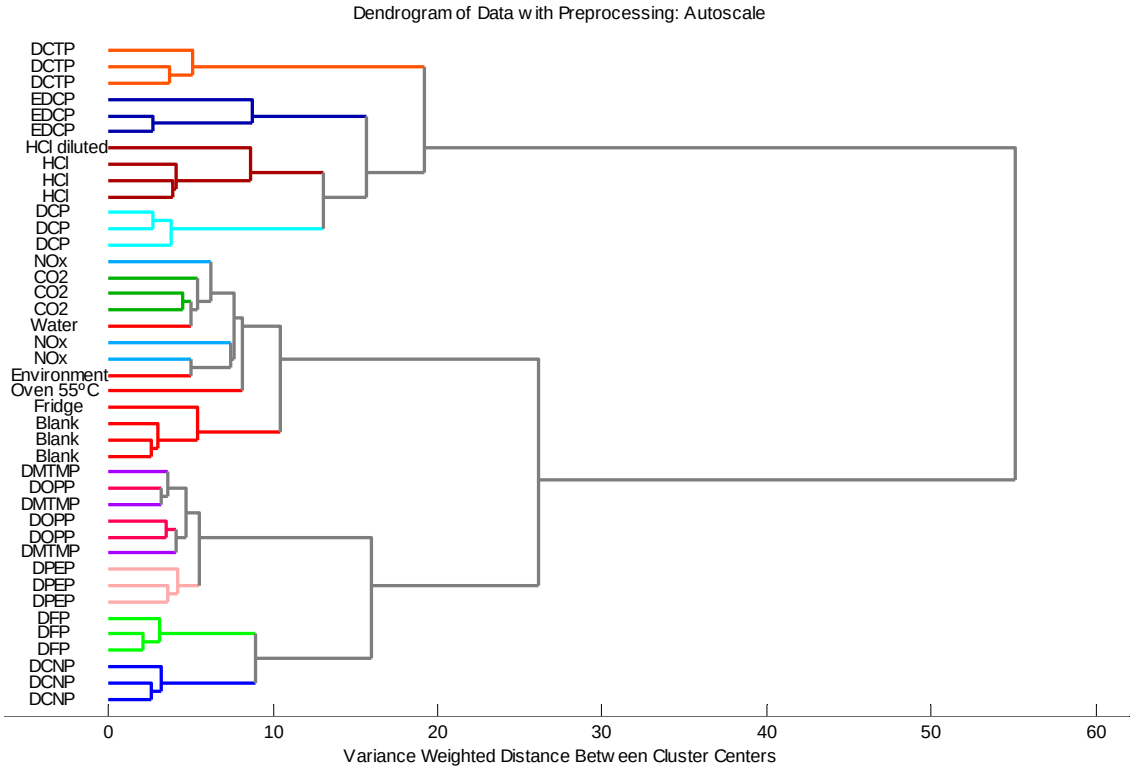

Figure S4. Dendrogram for 9 sampling organo- phosphate and phosphonate derivatives, blank samples and interferents as CO_2 and NOx showing Euclidean Distance with Ward Linkage.

K-nearest neighbour classifier (KNN) model

Confusion Matrix:

Class:	TP	FP	TN	FN
Blank	0.5714	0.0294	0.9706	0.4286
DCNP	1.0000	0.0000	1.0000	0.0000
DCP	1.0000	0.0263	0.9737	0.0000
DFP	1.0000	0.0000	1.0000	0.0000
HCl	1.0000	0.0000	1.0000	0.0000
Interferents	0.8333	0.0857	0.9143	0.1667
OrganoPhosphates	0.8333	0.0000	1.0000	0.1667
Phosphonates	1.0000	0.0000	1.0000	0.0000

TP: proportion of positive cases that were correctly identified
FP: proportion of negatives cases that were incorrectly classified as positive
TN: proportion of negatives cases that were classified correctly
FN: proportion of positive cases that were incorrectly classified as negative

Confusion Table:

Actual Class	Blank	DCNP	DCP	DFP	HCl	Interferents (CO_2 and NOx)	Organo-phosphates	Phosphonates
Predicted as								
Blank	4	0	0	0	0	1	0	0
DCNP	0	3	0	0	0	0	0	0
DCP	0	0	3	0	0	0	1	0
DFP	0	0	0	3	0	0	0	0
HCl	0	0	0	0	4	0	0	0
Interferents (CO_2 and NOx)	3	0	0	0	0	5	0	0
Organo-phosphates	0	0	0	0	0	0	5	0
Phosphonates	0	0	0	0	0	0	0	9
Total N	7	3	3	3	4	6	6	9
Ncorrect	4	3	3	3	4	5	5	9
Proportion	57%	100%	100%	100%	100%	83%	83%	100%
	N= 41		Ncorrect = 36			Proportion Correct= 88%		

Partial Least Square (PLS) studies:

A PLS model for prediction of the DFP concentration was created with the RGB colour coordinates obtained from the chromogenic array (vide infra). Concentrations of DFP of 108, 54, 44, 39 and 24 ppm (v/v) were tested. Figure S5 shows the PLS graph in which the measured vs. the predicted values of DFP concentrations ppm (v/v) were plotted. Hence the measured values represent the real DFP concentration, while the predicted values are calculated according to the PLS algorithm using the RGB data. Both the measured and predicted values were plotted together to evaluate the accuracy and precision of the created prediction model. Ideally, the predicted values should lie along the diagonal line, indicating in this case that the predicted and actual values are the same. The PLS prediction model for DFP concentrations shows a good agreement between the measured and predicted values suggesting that the array could display sensing of this hazard at concentrations of some few ppm.

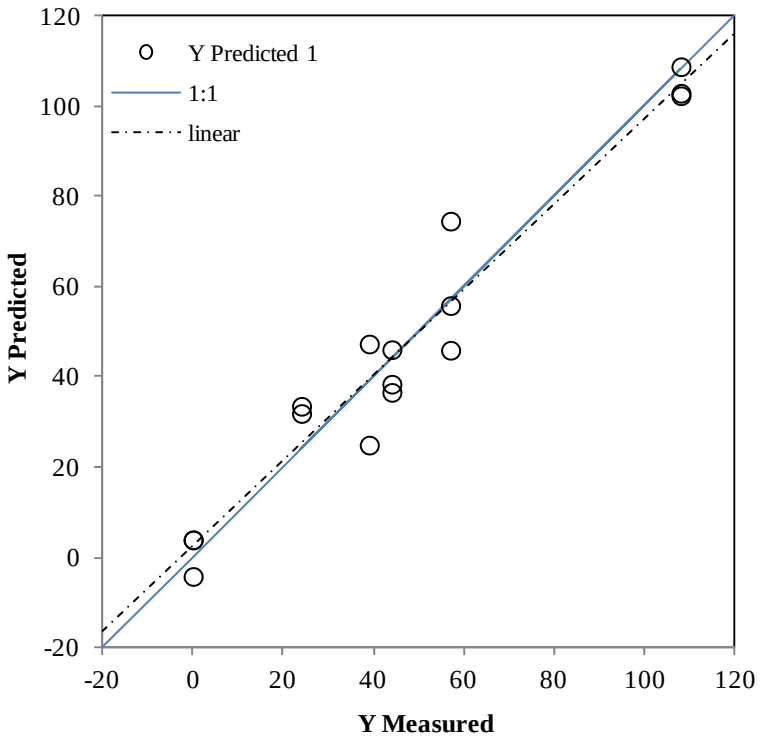

Figure S5. Experimental versus predicted values of DFP concentrations (ppm v/v) by using the PLS statistical model (dashed lines). The solid line represents the ideal behaviour.

References:

S1: S. Royo, R. Gotor, A. M. Costero, M. Parra, S. Gil, R. Martínez-Máñez, F. Sancenón, *New J. Chem.* **2012**, *36*, 1485.

S2: R. Gotor, A. M. Costero, S. Gil, M. Parra, R. Martínez-Máñez, F. Sancenón, *Chem. Eur. J.*, **2011**, *17*, 11994.

S3: H. Li, C.-H. Huang, Y.-F. Zhou, X.-S. Zhao, X.-H. Xia, T.-K. Li, J. Bai, *J. Mater. Chem.* **1995**, *5*, 1871.

S4: A. M. Costero, M. Parra, S. Gil, R. Gotor, R. Martínez-Máñez, F. Sancenón, S. Royo, *Eur. J. Org. Chem.* **2012** in press (DOI: 10.1002/ejoc.201200570).